doi: 10.5028/jatm.2012.04043012

Effect of Dielectric Barrier Discharge on the Airflow Around a Cylinder

Ashraf El Droubi*, Dawson Tadeu Izola
Escola de Engenharia de São Carlos, University of São Paulo – São Carlos/SP – Brazil

Abstract: *Fluids in a dielectric barrier glow discharge at atmospheric pressure have attracted interest from communities of thermo and fluid dynamics, as well as control. This work investigated the effects of a plasma actuator, operating at 8.0 kV and 4.4 kHz, on the pressure distribution around a polyvinyl chloride circular cylinder in low-velocity airflow. The experiment was repeated with the actuator at various angles. The results show an acceleration of the flow demonstrated by a 60% lower pressure coefficient at the actuator area. The flow separation was also delayed by an angle of as much as 30º. These effects were shown to be greater when the actuator was positioned at an angle closer to the separation area.*

Keywords: *Glow discharge, Dielectric barrier discharge, Flow control, Plasma actuator, Synthetic plasma jet.*

INTRODUCTION

The aerodynamic plasma actuator is a particular configuration of the dielectric glow discharge. The actuator consists of two thin electrodes asymmetrically installed that have a superior electrode exposed to the fluid flow and an inferior one. The two electrodes are separated by a thin sheet of insulating material, i.e., the dielectric, as shown in Fig. 1.

The electrodes of the plasma actuator are long and thin, installed spanwise along the aerodynamic body. When applying an electric potential of 5 to 20 kV across the electrodes with a frequency of 3 to 15 kHz, the actuator induces the formation of glow discharge plasma on the surface of the body along the electrode. The plasma particles are accelerated by the electric field of the actuator and then they collide with the neutral air particles around it. This can result in an exchange of momentum, which alters the flow around the body. The effect is perceived as a small jet along the body.

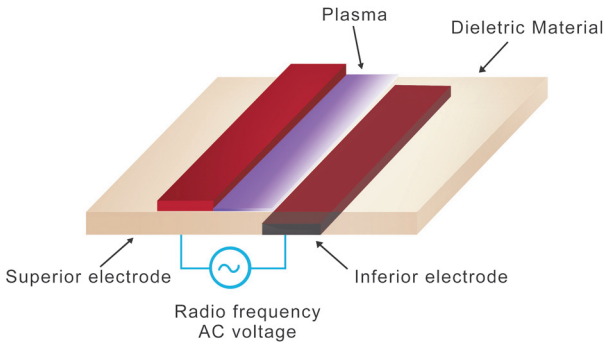

Figure 1. Illustration of the plasma actuator with the induced flow.

PREVIOUS WORK

Experiments found in literature are generally carried out on a flat plate. A direct current (DC) corona discharge was used for the first time by Malik *et al.* (1983) on a flat plate to manipulate the boundary layers, resulting in a drag reduction of about 20% for speeds up to 30 m/s with a 15 kV applied voltage. The efficiency of the actuator would mainly depend on the voltage used across the electrodes. Furthermore, drag reduction decreased with increasing flow velocity and with decrease in the potential difference between electrodes (el Khobairy and Clover, 1997). In later studies, glow discharge plasmas were used to control the flow boundary layer on flat plates, and it was observed that asymmetrical configurations of the electrodes produced more thrust than symmetrical ones, while an increase in drag was seen (Roth *et al.*, 2000). The effects were attributed to the combination of mass transport and vortex-induced electrohydrodynamic (EHD) forces. Some applications of the plasma actuators

Received: 15/05/12 Accepted: 26/09/12
*author for correspondence: ashraf.droubi@gmail.com
Departamento de Pós Graduação em Engenharia Mecânica,
Universidade de São Paulo.
Avenida Trabalhador São-Carlense, 400 – Parque Arnold Schmidt
CEP 13.566-590 São Carlos – SP/Brasil

have been investigated and include separation control of low Reynold's flow (Goksel *et al.*, 2006), improvement of airfoils (Corke *et al.*, 2002; 2006), virtual flaps and slats to control flow airfoil (Corke *et al.*, 2004), control of flow separation in low-pressure turbines (Rivir *et al.*, 2003), and noise reduction gear (Thomas *et al.*, 2005).

While most of these applications are restricted to incompressible flows, an application in high-speed flows has been reported as axisymmetric jet using plasma (Samimy *et al.*, 2004).

In later experiments performed by Enloe *et al.* (2004), several findings were presented on the behavior of the plasma actuators. Based on various measurements of pressure, voltage and plasma emission, the authors made several interesting conclusions: the input power (P) into the plasma is nonlinear with the voltage drop (ΔV); and the induced speed and thrust are proportional to the input power.

The final conclusion is that the plasma induces an electrostatic force, which can be treated as a body force, as opposed to a contact force, a body force operates throughout the body volume, around the fluid, proportional to the net charge density and strength of the electric field. It was also noted that the direction of flow-induced plasma can be altered/controlled by the arrangement of the electrodes.

Speed measurements induced at the beginning and end of discharge show that the ionic wind in a dielectric barrier discharge (DBD) actuator is generated periodically, indicating that the actuator does not behave the same in positive and negative parts of the cycle of the input AC voltage.

It has been seen that several attributes of the actuator, including the power and input voltages, input frequency, electrode geometry, orientation of the actuator, dielectric material, dielectric thickness, freestream, Re, pressure gradient, chemical composition of the plasma, and humidity are essential variables that determine the behavior of the actuator.

Porter *et al.* (2006) measured the thrust produced during the ongoing operation of a plasma actuator, and examined the effects of individual variables: the AC input voltage and frequency. It was concluded that the average body force is: linearly proportional to the input AC frequency between 5 and 20 kHz (for constant input voltage), and nonlinearly proportional with the input voltage (for a constant frequency).

Furthermore, the actuator 'pushes' (with a relatively higher magnitude) and 'pulls' (with a relatively lower magnitude) the fluid in opposite directions during each cycle.

Roth et Dai (2006) studied the effects of changing the dielectric material, electrode geometry, frequency and voltage applied to the flow velocity induced by the actuator. They observed that the choice of dielectric material affects the plasma volume, the distribution of electric field lines (governed by the dielectric constant), and heat loss, which, in turn, is proportional to the frequency of the alternating current input and the area electrode. In general, it is a material that has been recommended to combine the following properties: greater dielectric constant (aluminum, for example), greater dielectric strength (e.g. Kapton), and a lower thermal conductivity (for example, quartz, polytetrafluoroethylene – also known as Teflon).

If compared with quartz, polytetrafluoroethylene, which has high dielectric constant, high dielectric strength, and low thermal conductivity, was used to generate a higher speed and lower flow-induced energy input. It was used as the dielectric material for other studies. The width of the electrodes was chosen to have the greatest EHD effect. The horizontal separation distance between the edges of the upper and lower electrodes has been found to have a significant effect on the speed of the induced flow, and an optimal configuration was found having a separation of 1 to 2 mm. It was noted that by increasing the frequency and keeping the voltage constant, or vice versa, induced an increase in speed, which briefly stabilized, reaching a certain threshold and decreasing soon after.

VanDyken *et al.* (2004) also observed that a thick dielectric would be able to handle a higher input voltage, and this has an ideal specific frequency.

While most of the literature on flow control through the plasma is essentially experimental in nature, several methodologies for the numerical modeling of the plasma actuators were investigated. The majority of current models typically use EHD term body force to simulate the effect of an actuator on the external flow.

PLASMA GENERATION

The generation of the plasma is obtained with two electrodes coupled to one surface of the dielectric material that covers the airfoil. The electrodes are fixed on upper and lower sides (Fig. 2), where an electric field is applied with a potential and frequency of about 8 kV and 5 kHz, respectively.

Shyy *et al.* (2002) proposed that asymmetry should be introduced to the arrangement of the electrodes, and consequently that discharge structure plays a significant role in the generation of plasma (Fig. 3).

The plasma state is a result of the addition of sufficient

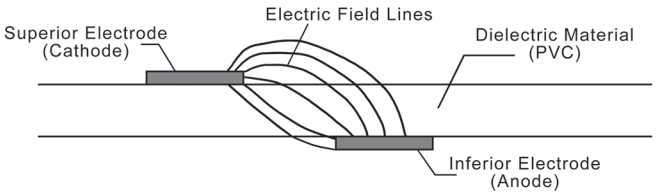

Figure 2. Electrode configuration showing the induced electric field lines (Shyy et al., 2002).

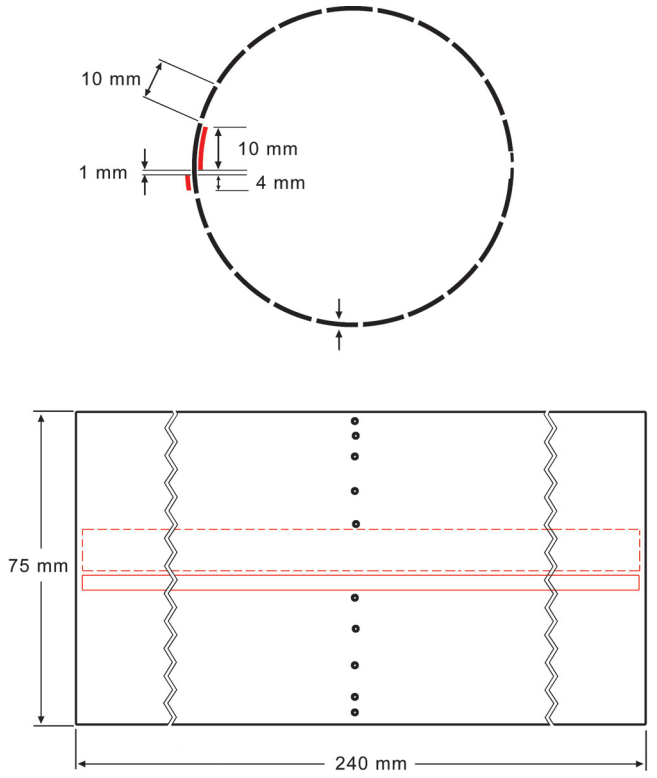

Figure 3. Schematic showing the lateral and front views of the cylinder with dimensions and position of the electrodes. The white spaces represent the pressure tubes.

energy quantities to a gas. The energy is added to dissociate the molecules of the gas. This is a result of collisions between particles whose energy exceeds the kinetic molecular energy.

Based on the amount of ionization, the plasma may be wholly or partially ionized. Weakly ionized plasma consists partly of ions and electrons and the gas of neutral particles, i.e. atoms and molecules. Our interest is in partially ionized gases. Plasma is also classified based on the temperature ranges. Low-temperature plasma can be classified as:

- thermal plasmas have electrons and heavy particles at the same temperature, i.e., they are in thermal equilibrium with each other;
- nonthermal plasmas on the other hand have the ions and neutrals at a much lower temperature (normally room temperature), whereas electrons are much 'hotter'.

High temperature plasmas are characterized by the kinetic temperature of electrons of $T_e \approx T > 10^7 K$, where T_e is the electron kinetic temperature and T is the overall temperature of the plasma. Low-temperature thermal plasmas are characterized by a value of $T_e \approx T < 2 \cdot 10^4 K$. Finally, nonthermal ones possess low temperatures of $T \approx 300K$ and $T_e < 10^5 K$.

The electric field that acts upon the charged particles, in particular on the electrons, is the main power source to the plasma. Due to the lower mass of electrons, only a small momentum transfer occurs with the heavier plasma particles and this is achieved by elastic collisions. Therefore, the electrons reach a mean kinetic energy level much higher than that of neutral particles, and the medium becomes nonthermal plasma. A significant portion of electrons is energetically able to overcome the threshold above which inelastic collisions occur. However, due to these inelastic collisions, the electrons lose excess energy that allowed the inelastic collisions, therefore they are transferred from a region of high kinetic energy to a low energy one. Thus, the population of electrons in the region of inelastic collisions decreases sharply with increasing power. This interaction between the action of the electric field and the processes of elastic and inelastic collisions causes the plasma to reach a state of thermodynamic equilibrium.

The electric field is stronger in the region closest to the inner edge of the two electrodes. Its electric force decreases as the distance of this region. It is logical that the probability of plasma formation is higher in the region of stronger electric fields. When the voltage increases, the electrons leave the cathode area and move towards the anode. These electrons collide with neutral particles and ions, causing additional ionization. It should be noted that this is not the surface of the anode, but the dielectric, which here represents a pseudoanode.

At the value of frequency mentioned, the electrons reach high speeds, leaving little time for atomic recombination, while the ions, which have relatively much less mobility, have no time to reach the electrode. Here, the flow rate is less than the frequency of discharge. This condition maintains a continuous discharge. Frequencies higher than 1 kHz are usually able to sustain it, while the periodicity is lost at lower frequencies.

In this work, the glow discharge created by the configuration assumes that the condition of quasi-neutrality is maintained as it is a basic property in technological plasmas and low energy DBDs.

METHODOLOGY

The experiment was conducted using a 75 mm PVC cylinder, and with electrodes installed as shown in Fig. 3. PVC is a good dielectric with a relatively low dielectric constant of 4.5 and a high dielectric resistance of 40 MV/m. The cylinder has 23 pressure tubes connected along its circumference. The tubes have 1 mm diameter each and are 10 mm apart. The upper and lower electrodes have a width of 4 and 10 mm, respectively, both having a 0.1 mm thickness. The electrodes are considered thin enough in order to not have any considerable effect on the flow.

The pressure tubes are connected to an electronic pressure measuring device SCANIVALVE, model D. The measurements were recorded with a precision of 0.003 V at a frequency of 1000 measurements/second over two seconds giving a total of 2,000 measurements per point.

Dividing the difference in the static pressure around the cylinder with that of the wind tunnel by the dynamic pressure of the tunnel, it results in the pressure distribution about the cylinder (Eq. 1).

Repeating the same procedure with the connected actuator demonstrates the effect of the interaction of the plasma flow, resulting in a modified Cp curve that is compared with the initial Cp curve with the actuator off. The process is repeated with the actuator positioned at the following angles: 0º, 60º, 70º, 80º, 90º, 100º, 110º, 120º, and 180º.

Experimental conditions

In the chosen configuration of the electrodes in this experiment, the optimal frequency was found around 4.4 kHz, which is determined when the power source presents the highest current drawn by the electrodes.

This frequency coincided with a brighter discharge accompanied with a higher discharge noise from the actuator: temperature of 22° Celsius; atmospheric pressure of 92,259.072 Pa; and relative humidity of 70%.

The lowest speed allowed by the wind tunnel was 3.93 m/s, at which the experiment was conducted and monitored in a test chamber of 400 x 300 x 200 mm. The experiment was conducted with a discharge of 8 kV and a frequency of 4.4 kHz providing the further results.

The pressure coefficient Cp is defined as the difference in static pressure between the flow over the airfoil and the free-flow in relation to the dynamic pressure of the free stream flow, as in Eq. 1:

$$C_p = \frac{(P_\theta - P_\infty)}{\frac{1}{2}\rho U_\infty^2} = \frac{(P_\theta - P_\infty)}{(P_T - P_\infty)} \quad (1)$$

where:
$(P_T - P_\infty)$: is the dynamic pressure;
P_θ is the static pressure;
P_T total pressure of the free stream;
P_∞ is the free stream static pressure.

This expression of Cp can be written as Eq. 2:

$$C_p = 1 - \left(\frac{v}{v_\infty}\right)^2 \quad (2)$$

Resulting in a flow velocity of (Eq. 3):

$$V = V_\infty \sqrt{1 - C_p} \quad (3)$$

For a free stream velocity of 3.92 m/s, in the case of no plasma, there was a C_p -1.5 at the point of maximum actuation, which correlated with a flow rate of $V = 3.92\sqrt{1 + 1.5} = 6.2$m/s.

With the actuator on, we noticed a greater negative C_p, a higher value of -2.5 when the actuator is positioned at 90º. The flow speed accelerating the actuator can be calculated by the same equation resulting in: $V = 3.92\sqrt{1 + 2.5} = 7.2$m/s.

Hence, we can conclude that the actuator was able to accelerate the flow by inducing a jet of 1 m/s.

EXPERIMENTAL OBSERVATIONS

Throughout the experiment, the electrodes demonstrated some physical degradation with use. Excluding excessive voltage applied to electrodes, actuator failures appeared to be due to degradation of the electrodes. The sudden failure of the actuator during the experiment was not unusual, even when stable voltage and frequency were maintained. The actuator failure was always presented as electric arcs shooting out of the edge of the actuator thus shorting the electrodes.

One form of physical degradation was the erosion of the exposed copper electrode. After prolonged use, the actuator presented an erosion of the electrode exposed to the side of the plasma-forming region. The electrode had a smooth edge before the operation and an irregular appearance after use. Another type of degradation is a discoloration on the surface of the dielectric downstream of the exposed electrode.

Several visual observations were made about the plasma appearance during operation of the actuator. Depending on the frequency and voltage, the discharge appears diffuse and becomes filamentary (multipoint Plasma concentration) with

an increase in both voltage and frequency. The transition of the discharge mode to filamentary depends on the spacing between the electrodes, dielectric thickness, and dielectric material. The filamentary discharge occurs when filamentary hot spots appear in the plasma, which appear to be brighter than other regions of the plasma due to the increased plasma formation in these regions.

When the discharge was filamentary, increasing the actuator operation frequency, while constant voltage was maintained, it resulted in an increased number of hot spots in the plasma. With the actuators used in this study, the presence of hot spots also typically indicated that the voltage applied to the actuator was near the maximum permitted by the dielectric. Therefore, the increase in voltage beyond this point resulted in a failure due to arcing-induced burns of the dielectric material (Fig. 4).

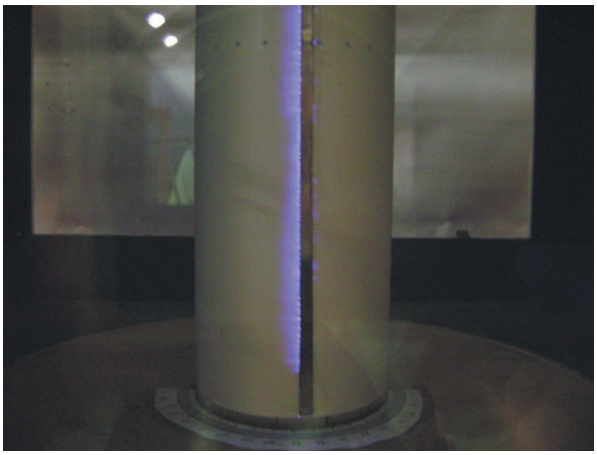

Figure 4. A filamentary discharge with various hot spots along the electrode.

RESULTS AND DISCUSSION

The results presented in this section are the average curves of Cp calculated at each angle of the actuator. The error is calculated with an interval of confidence of 90% and is shown in bars at various points on the curves. The position of the actuator relative to the cylinder is presented by a vertical dotted line (Fig. 5).

Positioning the actuator in the stagnation point of the cylinder does not result in a considerable effect. The C_p curve is almost identical for the flow with and without plasma with minor differences in the region of turbulence. Notice that this region is very turbulent and the pressure gradient varies greatly, resulting in fluctuations in the curve of C_p. Also, observe that the error value of the two curves overlap, which shows some confidence in the values obtained in the experiment (Fig. 6).

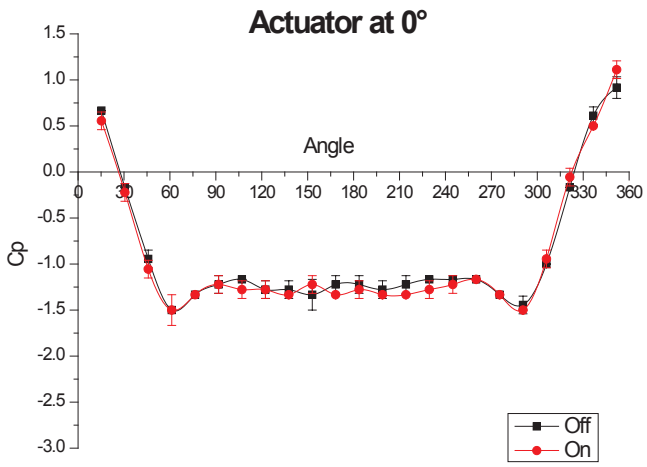

Figure 5. C_p curve with the actuator both on and off. Actuator positioned at 0º.

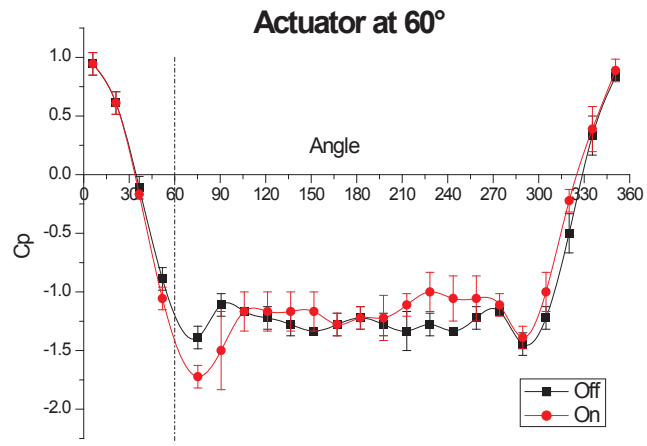

Figure 6. C_p curve with the actuator both on and off. Actuator positioned at 60º.

Positioned at 60°, the actuator demonstrates a small effect; however, it is clear and identified. An acceleration of the flow can be inferred from the graph, with C_p reaching -1.7, and there is a greater pressure recovery. There was also a delay of the point of separation to about 10° (Fig. 7).

At 70°, the actuator provides a greater effect. The acceleration of the flow results in a value of -1.85 for C_p. The separation point is also shifted nearly 10° to the trailing edge of the cylinder. This effect is not encountered on the other side of the cylinder, which does not have an actuator; here, the C_p curve is almost identical with the actuator turned off.

The actuator shows a greater effect when positioned at 80° (Fig. 8). Therefore, the acceleration of the flow changes the pressure coefficient at this point to -2.5 C_p. The displacement of the flow's separation point surpasses an angle of 10°.

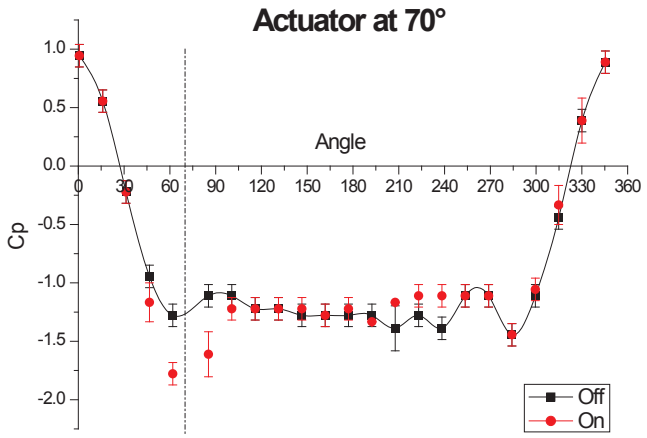

Figure 7. C_p curve with the actuator both on and off. Actuator positioned at 70º.

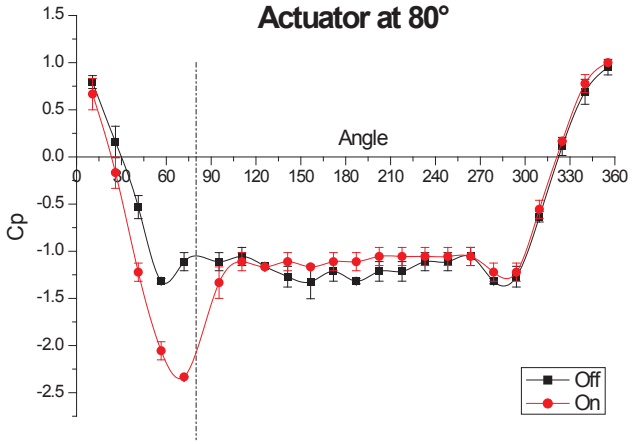

Figure 8. C_p curve with the actuator both on and off. Actuator positioned at 80º.

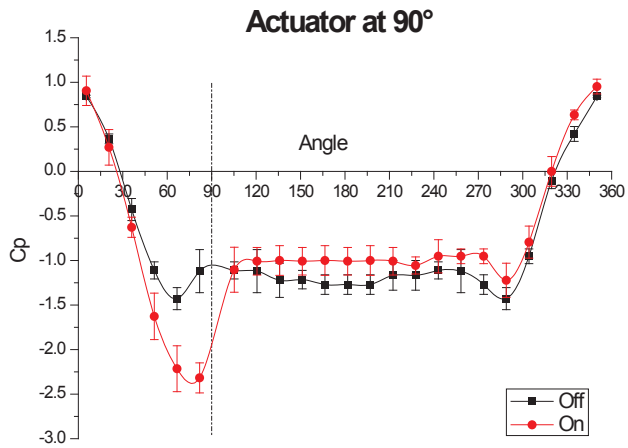

Figure 9. C_p curve with the actuator both on and off. Actuator positioned at 90º.

At 90°, the acceleration reaches the maximum allowed by the actuator (Fig. 9). There was a relatively high recovery of C_p reaching -1. The separation point moves back to 15°. There is a worth noting small deceleration on the other side of the cylinder. The turbulent region with the actuator on shows higher values of C_p than that with the actuator off. We can thus infer that the actuator caused a decrease in drag by diminishing the wake size (Fig. 10).

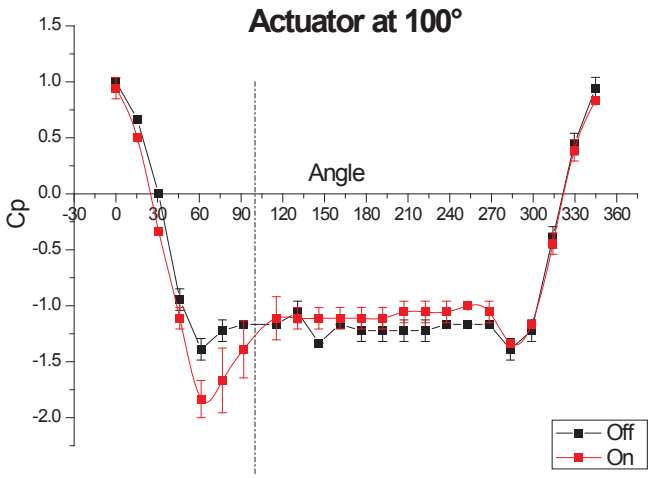

Figure 10. C_p curve with the actuator both on and off. Actuator positioned at 100º.

The actuator continues to present an effect after 90°. However, less than that of 90°, the actuator placed at 100° was able to accelerate the flow by pulling the C_p value to -1.9. It is interesting to note that the separation point showed a shift of about 30° when the actuator was placed right after the separation point (Fig. 11).

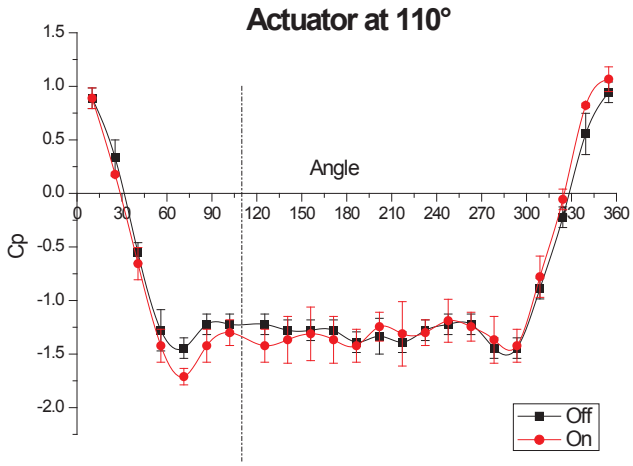

Figure 11. C_p curve with actuator both on and off. Actuator positioned at 110º.

Continuing to 110°, the effect of the actuator decreases but still causes a small acceleration, similar to when the actuator is at 60° (Fig. 12).

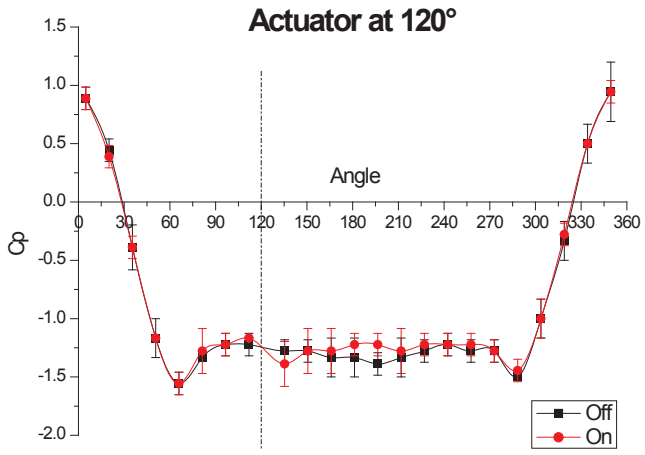

Figure 12. C_p curve with the actuator both on and off. Actuator positioned at 120º.

With a larger angle, the actuator ceases to have an observed effect. The C_p curve with the actuator on was almost identical with it off (Fig. 13).

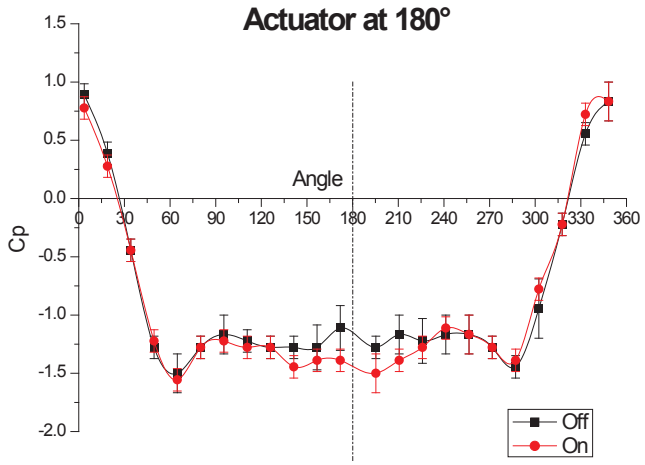

Figure 13. C_p curve with the actuator both on and off. Actuator positioned at 180º.

At 180°, the actuator did not show any observable effect.

CONCLUSIONS

The results show a tangible effect of using the plasma actuator. The actuator induced a remarkable acceleration in the flow over a cylinder varying with its angle with respect to the flow. The angles with greatest interaction related to the flow are those close to the point of separation. The actuator gradually loses ability to induce a change in the flow the further it is placed from the point of separation. The delay in the flow separation is also a result of the higher suction induced by the low pressure created by the actuator. It is important to note that at angles slightly past the separation point, the actuator, despite inducing a relatively lower acceleration, could further delay the separation by up to 30°.

In this experiment, the interaction of glow discharge plasma with airflow was demonstrated and confirmed. The actuator achieved a clear acceleration of the flow shown by a 60% lower C_p. Also, the actuator induced a delay in the separation of the flow by 30°. However, it showed a greater effect when located in the region of separation, presenting decreasing efficiency with further placement from this region. These results show a capacity to generate more lift and less drag, making the actuator a good control device. This makes plasma actuators quite attractive in the area of aerodynamic research. We can conclude from the data obtained that the plasma actuator has a substantial and positive effect on the flow over an airfoil. This presents many opportunities and situations in which the actuator can be used in the future, and deserves to be further researched.

REFERENCES

Corke, L. and Post, M., 2005, "Overview of plasma flow control: concepts, optimization, and applications", 43rd AIAA Aerospace Sciences Meeting and Exhibit, Reno, NV: AIAA.

Corke, T.C. *et al.*, 2006, "Plasma flow control optimized airfoil", 44th AIAA Aerospace Sciences Meeting and Exhibit, Reno, NV: AIAA.

Corke, T.C. *et al.*, 2004, "Plasma flaps and slats: an application of weakly ionized plasma actuators", 2nd AIAA Flow Control Conference, p. 2127, Portland, OR: AIAA.

Corke, T.C. *et al.*, 2002, "Application of weakly-ionized plasmas as wing flow-control devices", 40th AIAA Aerospace Sciences Meeting and Exhibit, Reno, NV: AIAA.

El-Khabiry, S. and Colver, G., 1997, "Drag reduction by dc corona discharge along an electrically conductive flat plate for small Reynolds number flow", Physics Fluids, Vol. 9, p. 587-599.

Enloe, C.L. *et al.*, 2004, "Plasma structure in the aerodynamic plasma actuator", 42nd AIAA Aerospace Sciences Meeting and Exhibit, Reno, NV: AIAA.

Goksel, B. *et al.*, 2006, "Steady and unsteady plasma wall jets for separation and circulation control", 3rd AIAA Flow Control Conference, San Francisco, CA: AIAA.

Hultgren, L. and Ashpis, D., 2003, "Demonstration of separation delay with glow-discharge plasma actuators", 41st AIAA Aerospace Sciences Meeting and Exhibit, Reno, NV: AIAA.

Lieberman, M.A. and Lichtenberg, A.J., 2005, "Principles of Plasma Discharges and Materials Processing", 2nd ed., Wiley-Interscience, pp. 43-63, 535-568.

Malik, M. *et al.*, 1983, "Ion wind drag reduction", 21st AIAA Aerospace Sciences Meeting and Exhibit (Reno, NV) AIAA Paper 83-0231.

Porter, C.O. *et al.*, 2006, "Temporal force measurements on an aerodynamic plasma actuator", 44th AIAA Aerospace Sciences Meeting and Exhibit, Reno, NV: AIAA.

Rivir, R. *et al.*, 2003, "Turbine Flow Control, Plasma Flows", 41st AIAA Aerospace Sciences Meeting and Exhibit, p. 6055, Reno, Nevada, USA: AIAA.

Roth, J.R. *et al.*, 2000, "Electrohydrodynamic Flow Control with a Glow Discharge Surface Plasma", AIAA Journal, Vol. 38, No. 7, July 2000, pp. 1166-1172.

Roth, J.R. and Dai, X., 2006, "Optimization of the aerodynamic plasma actuator as an electrohydrodynamic (ehd) electrical device", 44th AIAA Aerospace Sciences Meeting and Exhibit (Reno, NV) AIAA, Paper 2006-1203.

Samimy, M. *et al.*, 2004, "Active control of high speed jets using localized arc filament plasma actuators", 2nd AIAA Flow Control Conference, Portland, OR: AIAA.

Shyy, W. *et al.*,2002, "Modeling of glow discharge-induced fluid dynamics", Journal of Applied Physics, Vol. 92, pp. 6434-6443.

Thomas, F.O. *et al.*, 2005, "Plasma actuators for landing gear noise reduction", 11th AIAA/CEAS Aeroacoustics Conference, Monterey, CA: AIAA.

VanDyken, R.D. *et al.*, 2004, "Parametric investigations of a single dielectric barrier plasma actuator", 42nd AIAA Aerospace Sciences Meeting and Exhibit, Reno, NV: AIAA.